AFRL-RZ-WP-TP-2012-0118

IN-SITU APPROACH TO INTRODUCE FLUX PINNING IN YBCO (POSTPRINT)

T.J. Haugan

Mechanical Energy Conversion Branch
Energy/Power/Thermal Division

FEBRUARY 2012

AIR FORCE RESEARCH LABORATORY
PROPULSION DIRECTORATE
WRIGHT-PATTERSON AIR FORCE BASE, OH 45433-7251
AIR FORCE MATERIEL COMMAND
UNITED STATES AIR FORCE

REPORT DOCUMENTATION PAGE

Form Approved
OMB No. 0704-0188

1. REPORT DATE *(DD-MM-YY)*	2. REPORT TYPE	3. DATES COVERED *(From - To)*
February 2012	Journal Article Postprint	04 April 2005 – 04 April 2007

4. TITLE AND SUBTITLE
IN-SITU APPROACH TO INTRODUCE FLUX PINNING IN YBCO (POSTPRINT)

5a. CONTRACT NUMBER
In-house

5b. GRANT NUMBER

5c. PROGRAM ELEMENT NUMBER
62203F

6. AUTHOR(S)
T.J. Haugan

5d. PROJECT NUMBER
3145

5e. TASK NUMBER
32

5f. WORK UNIT NUMBER
314532ZE

7. PERFORMING ORGANIZATION NAME(S) AND ADDRESS(ES)
Mechanical Energy Conversion Branch (AFRL/RZPG)
Energy/Power/Thermal Division
Air Force Research Laboratory, Propulsion Directorate
Wright-Patterson Air Force Base, OH 45433-7251
Air Force Materiel Command, United States Air Force

8. PERFORMING ORGANIZATION REPORT NUMBER
AFRL-RZ-WP-TP-2012-0118

9. SPONSORING/MONITORING AGENCY NAME(S) AND ADDRESS(ES)
Air Force Research Laboratory
Propulsion Directorate
Wright-Patterson Air Force Base, OH 45433-7251
Air Force Materiel Command
United States Air Force

10. SPONSORING/MONITORING AGENCY ACRONYM(S)
AFRL/RZPG

11. SPONSORING/MONITORING AGENCY REPORT NUMBER(S)
AFRL-RZ-WP-TP-2012-0118

12. DISTRIBUTION/AVAILABILITY STATEMENT
Approved for public release; distribution unlimited.

13. SUPPLEMENTARY NOTES
Journal article published as a chapter in Flux Pinning and AC Loss Studies in YBCO Coated Conductors. Work on this effort was completed in 2007. This is the best quality available of this publication. Paper contains color.

 PA Case Number: AFRL/WS-06-0738; Clearance Date: 04 Apr 2007.

14. ABSTRACT

Several in-situ methods to introduce ultra-high densities of defects into YBCO to enhance flux pinning are reviewed, including rare-earth or chemical substitution or additions, and nanoparticle additions by various processing methods. The results were compiled using studies published recently or that are publicly available. Superconducting and microstructural properties are compared for different nanoparticle additions including Y211, Y_2O_3, CeO_2, Sm123, MgO, La211, $IrZO_3$, $BaZrO_3$, and mixed (Y,RE)123 compositions. Results are included for thin films deposited on single crystals and metallic substrates, and for bulk powders. Of the methods reviewed, only processing conditions that produced nanoparticle additions have demonstrated significant $J_c(H)$ enhancements for high fields $H_{appl}>0.3T$, whereas rare-earth-only substitutions have increased $J_c(H)$ at low-fields $H_{appl}<1T$ in the case when secondary nanoparticles formations were not observed. For nanoparticle additions high-lattice mismatch materials have given consistently large increase of $J_c(H)$. Results with small-lattice mismatched materials are less consistent thus far; several groups are reporting increases of $J_c(H)$ with large $(Y,X)_2O_3$-type nanoparticle size about ~15 nm to ~40 nm, whereas other groups are reporting minimal results with small $(Y,X)_2O_3$-type nanoparticle sizes ~5 nm. In this work, very-small lattice mismatches degraded flux pinning presumably by making Y123 more uniform and with less pinning defects.

15. SUBJECT TERMS
compositions, nanoparticle, substrates, metallic, enhancements, processing, in-situ, superconducting, microstructural

16. SECURITY CLASSIFICATION OF:			17. LIMITATION OF ABSTRACT:	18. NUMBER OF PAGES	19a. NAME OF RESPONSIBLE PERSON (Monitor)
a. REPORT	b. ABSTRACT	c. THIS PAGE			Timothy J. Haugan
Unclassified	Unclassified	Unclassified	SAR	26	19b. TELEPHONE NUMBER *(Include Area Code)* N/A

In: Flux Pinning and AC Loss Studies on YBCO… ISBN: 978-1-60021-692-3
Editors: M. P. Paranthaman et al., pp. 59-77

Chapter 4

IN-SITU APPROACH TO INTRODUCE FLUX PINNING IN YBCO

T. J. Haugan*
Air Force Research Laboratory, Wright-Patterson AFB,
OH 45433-7251 U.S.A.

ABSTRACT

Several in-situ methods to introduce ultra-high densities of defects into YBCO to enhance flux pinning are reviewed, including rare-earth or chemical substitution or additions, and nanoparticle additions by various processing methods. The results were compiled using studies published recently or that are publicly available. Superconducting and microstructural properties are compared for different nanoparticle additions including Y211, Y_2O_3, CeO_2, Sm123, MgO, La211, $IrZO_3$, $BaZrO_3$, and mixed (Y,RE)123 compositions. Results are included for thin films deposited on single crystals and metallic substrates, and for bulk powders. Of the methods reviewed, only processing conditions that produced nanoparticle additions have demonstrated significant $J_c(H)$ enhancements for high fields $H_{appl} > 0.3$ T, whereas rare-earth-only substitutions have increased $J_c(H)$ at low-fields $H_{appl} < 1$T in the case when secondary nanoparticles formations were not observed. For nanoparticle additions high-lattice mismatch materials have given consistently large increase of $J_c(H)$. Results with small-lattice mismatched materials are less consistent thus far; several groups are reporting increases of $J_c(H)$ with large $(Y,X)_2O_3$-type nanoparticle size about ~15 nm to ~40 nm, whereas other groups are reporting minimal results with smaller $(Y,X)_2O_3$-type nanoparticle sizes ~5 nm. In this work, very-small lattice mismatches degraded flux pinning presumably by making Y123 more uniform and with less pinning defects. TEM of high-lattice mismatch nanoparticles additions indicates stress regions surrounding the nanoparticles can extend out to 10-15 nm size. The combined studies strongly suggest that stress-related defect zones and/or large nanoparticles size > 10 nm are critically important to achieve significant increases of flux pinning for high-field H > 1T, whereas smaller nanoparticles sizes are not as effective for these field strengths.

* T. J. Haugan: E-mail: timothy.haugan@wpafb.af.mil

1. INTRODUCTION

Since the discovery of high temperature superconductors (HTS) in 1986 and 1987 [1,2], there has been continual interest in increasing the critical current density (J_c) of these materials in practical forms including wires, thin films and bulk materials. To increase the J_c of HTS type-II superconductors in applied magnetic fields, it is well-understood method that non-superconducting defects must be incorporated into the superconducting materials to act as extended pinning centers for the magnetic fluxons that penetrate the superconductor [3-5]. The size of the pinning defects is preferred to be of the order of the coherence length, which is ~ (2-4) nm for $YBa_2Cu_3O_{7-\delta}$ (YBCO) in the temperature range (4-77) K. A small size of defect is sufficient to pin the vortices and also allows a higher pinning defect density to be reached. An areal density of about $H/2x10^{11}$ defects/cm^2 is desired to pin every fluxon in an applied field of H in units of Tesla [3-5].

Methods of defect addition can be classified as in-situ methods which directly add defects into the superconductor during processing, or ex-situ methods which incorporate the defects after processing. Ex-situ methods can include irradiation [5] or mechanical methods such as stressing which can influence twin-defect densities [6]. Herein focuses on in-situ methods of defect addition by selected approaches. The in-situ method is arguably the most practical method to consider for industrial applications, since estimates for ex-situ irradiation processes are generally high because of expensive in-line beam-use costs. The $YBa_2Cu_3O_{7-x}$ (YBCO or Y123) superconductor is reviewed in this chapter since it is the primary conductor being developed presently for coated conductor applications [7-14].

2. RARE-EARTH OR CHEMICAL SUBSTITUTIONS OR ADDITIONS

A conceptually simple and cost-effective method of adding nanosize pinning centers is to dope or partially introduce different elements directly into the lattice structure, which changes the properties of the localized areas in and around such doped crystal structures. Chemical substitution into RE123 with rare-earth cations has been studied by many groups recently [15-59]. The substitution of chemical elements into the $YBa_2Cu_3O_{7-\delta}$ (YBCO or 123) superconductor has been studied extensively and summarized for crystal growth [37], doping and physical properties [38], and materials chemistry and thermodynamics [39]. Recently the effects on flux pinning and $J_c(H)$ properties were reviewed [40], however more specific results are summarized and updated herein. A potential difficulty with rare-earth substitutions is that the higher ionic radii RE123 materials have significantly higher melting points than YBCO, which may require higher processing temperatures that may not be compatible with the present CeO_2/YSZ/Y_2O_3/RABIT's Ni structure optimized for YBCO commercial production [7-11].

Different variations of RE doping have been studied, including substitution in (Y,RE)123 with RE = Ho, Dy, Gd, Eu, Nd, and Pr, and various other combinations of rare-earths such as mixed (RE_1,RE_2)123 or (RE_1,RE_2,RE_3)123 compositions such as (Nd,Eu,Gd)123 [15-59]. Recent studies have demonstrated that significant increases of $J_c(H)$ can be achieved in mixed RE123 materials and particularly for RE ~ 0.33 or ~0.66 in (Y,RE)123 compositions; e.g. for RE = Ho, Gd, Dy, Sm, and Eu [33,46-49,40], and for mixed ($Nd_{0.333}$,$Eu_{0.333}$,$Gd_{0.333}$)123

[21,40]. At least 150 papers have been published on (Y,RE)123 flux pinning, however there tends to be limited systematic studies on $(Y_{1-x}RE_x)123$ for the complete range of $x = 0 - 1$ [40].

Possible mechanisms by which RE substitutions can increase flux pinning include: (a) addition of second-phase defects by precipitation or composition changes, (b) formation of finely distributed lower T_c components from the mixed solubility of RE with Ba and intersolubility of RE or other mechanisms, (c) randomly distributed oxygen-deficient zones which have lower T_cs [21,22], or (d) intrinsic stresses resulting from the lattice mismatched RE123 agglomerations [35,36]. The finely distributed lower T_c components are suggested as a cause of the so-called "fish-tail" effect, where as the magnetic field is increased, the J_c temporarily increases as the lower T_c components transition to normal behavior after which the J_c decreases at much higher applied magnetic fields [21,22,43]. The peak of the J_c maximum in these materials typically occurs at applied fields of about 2 T to 3 T, and the "fish-tail" peaks been observed in melt-processed (Y,Gd)123 [43]. The distribution and size of the RE123 unit cell agglomerations is not precisely known, however presumably would variably affect the T_c and $J_c(H)$ properties.

The effect of RE substitution on the superconducting transition temperature (T_c) is reviewed in figure 1 for both thin films and bulk materials. In general T_c increases with increasing RE substitution for (Y,RE)123 especially for bulk materials, as expected for the trend of increasing T_c for RE123 with higher ionic radii [37-40]. The trend of increasing T_c was more consistently observed for bulk materials, however was also measured in thin films. Interestingly, there is a noticeable dip or lack of increase around RE = 0.2 reported by several authors in bulk materials for Gd and Eu [31,50,53,59], and discussed in detail by one author [50].

For thin films the substrate can have a large effect on the T_cs which presumably affects the results in figure 1 [54-56]. Recently this was confirmed for (Y,Eu)123 films deposited onto varying substrates including $SrTiO_3$, $LaAlO_3$, LSAT and CeO_2-YSZ films [57]. A flat dependence of T_c on Eu substitution was observed for films deposited onto $LaAlO_3$ $SrTiO_3$ or LSAT substrates similar to (Y,Dy)123 films deposited on $LaAlO_3$ shown in figure 1. However for (Y,Eu)123 films deposited on CeO_2-YSZ in figure 1, a nearly linear dependence of T_c with Eu substitution was measured which is markedly different [57].

The effect of RE substitution on critical current density (J_c) is reviewed in figure 2 for thin films and in figure 3 for bulk materials. The effect on J_c is plotted for different applied fields from 0 T to 3 T. The relative increase of J_c depends specifically on the applied field; e.g. for (Y,Eu)123 films an increase of J_c for Eu substitution occurs for $H < 1$ T, however J_c decreases with Eu substitution for $H > 1$T [57]. Especially for $H_{appl} = 0.1$ T, a fairly consistent trend is observed in figure 2 that J_c increases significantly about 2 times with increasing RE substation. Only for RE = Dy was a peak around RE = 0.3 observed in these studies, compared to the peak observed from various RE combinations observed by several groups [21,33,46-49,40]. The decrease of (Y,Dy)123 films with higher $H_{appl} > 0.5$ T compared to (Y,Eu)123 films is probably a consequence of different measuring magnetic measurement measurements: for (Y,Dy)123 films SQUID was used which typically has a slow ramp rate [49], whereas as for (Y,Eu)123 films VSM was used with a (generally) higher ramp rate of 100 Oe/sec (7900 A/m•s) [57].

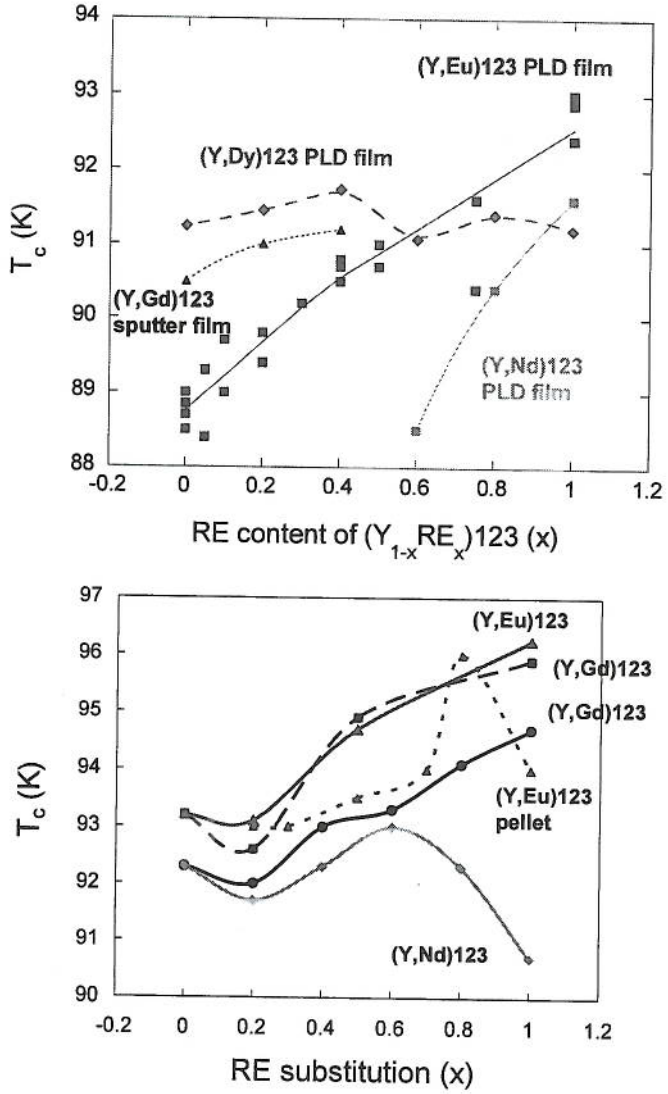

Figure 1. Effect of RE substitution on the transition temperature of (Y,RE)123 superconductors: (top) thin films (Y,Dy)123 on $LaAlO_3$ [49], (Y,Eu)123 on $CeO_{2\text{-buffer}}$-YSZ [57], (Y,Gd)123 on STO or YSZ [46], and (Y,Nd)123 on $LaAlO_3$ [58], and (bottom) bulk powders RE =(Y,Eu)123 dashed-lines [50], (Y,Eu)123 solid-lines [53], (Y,Gd)123 dashed-lines [53], (Y,Gd)123 solid-lines [59], and (Y,Nd)123 [31,59].

The effect of RE substitution on J_c(77K) of bulk materials is shown in figure 3. Enhancements of J_c with RE substitution for low-fields H < 1T were observed for RE = Gd and Eu, however at high fields H > 3 T improvements were also measured for RE = Nd in addition. A peak in J_c was measured for Eu = 0.3 and Eu = 0.7 in bulk powders, but could not be reproduced in thin films (figure 2).

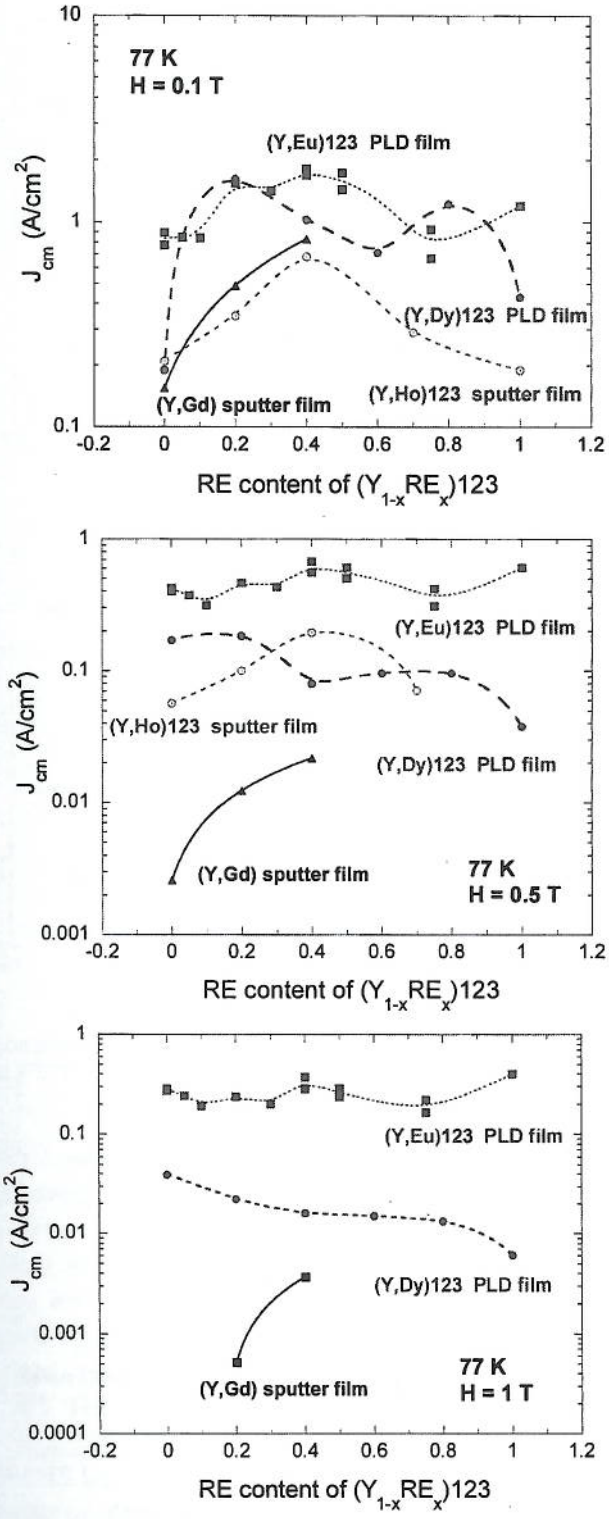

Figure 2. Effect of RE substitution on $J_c(H)$ properties of thin films for RE = Dy [49], Eu [57], Gd [46], and Ho [48]; for H_{appl} // c-axis = 0.1 to 1 T from top to bottom. Critical current density was measured by magnetic methods (J_{cm}).

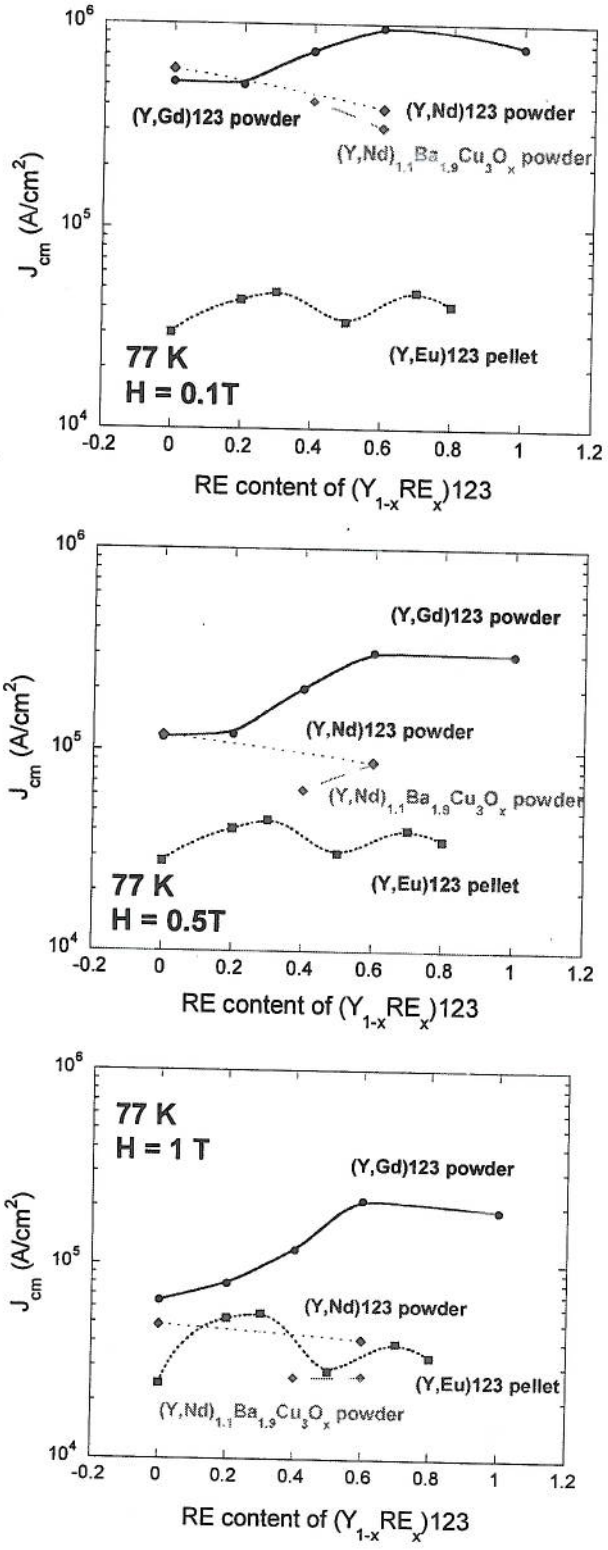

Figure 3. Continued on next page.

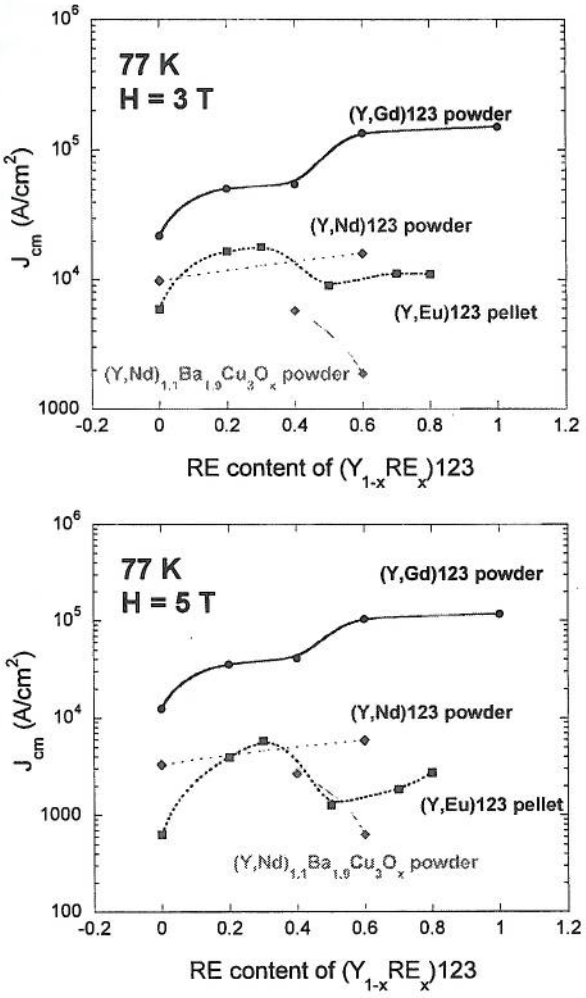

Figure 3. Effect of RE substitution on $J_c(H)$ properties of bulk samples for RE = Eu [50], Gd [59], and Nd [31] for H_{appl} = 0.1 T to 5 T from top to bottom. Critical current density was measured by magnetic methods (J_{cm}).

The difference in J_{cm} magnitudes comparing RE = Eu to Nd or Gd in figure 3 probably result from different interpretations of the particle size used for the Bean model [50,59]. Other differences in $J_c(H)$ were measured at 65K for bulk powders [59], indicating that care must be used to exactly measure and compare flux pinning properties at specific temperatures.

The effect of the RE variance and RE ion-size substitutions was studied recently by MacManus-Driscoll et. al. by changing the RE ion-size variance while holding the RE ion-size constant [33], and reverse studies varying the RE ion-size holding the RE ion-size variance constant [34]. They found that for constant RE ion-size, a consistent trend was observed for low-field $J_c(0.2T)$ decreasing with increasing RE ion-size variance [33]. However for constant RE ion-size variance, no trends were observed for varying RE ion-size [34]. The enhancements of J_c versus variance for constant RE ion-size are plotted in figure 4, and compared to recent results of (Y,Eu)123 substitutions. Interestingly, the results are

different for Eu substitution, suggesting that microstructural issues are also affecting these results. In figure 4, the average RE ion size and variance were calculated using

$$\text{RE ave} = \Sigma\, x_i * r_i \text{ and}$$

$$\sigma^2 = \Sigma\, x_i \langle r_i \rangle^2 - \langle \text{RE ave} \rangle^2$$

where i = ionic ion, x = RE mole fraction of normalized to 1, and r is ionic radii of VIII Coordination Number +3 valence state.

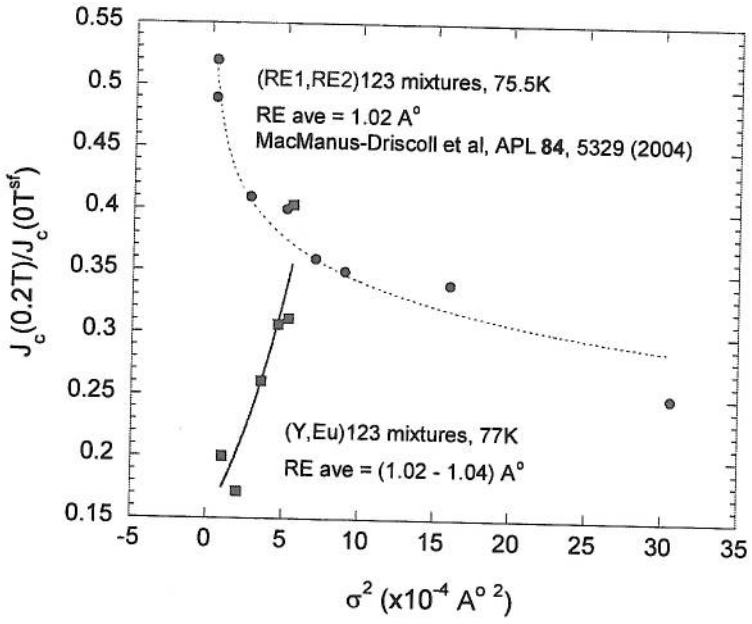

Figure 4. The effect of low-field J_c enhancements as a function of RE variance for (RE1,RE2)123 mixtures with J_c measured by transport method [33], compared to similar studies with (Y,Eu)123 measured by magnetic methods [57]. The difference of J_c measurements methods is not expected to have much effect on these studies, especially when J_c is normalized to self-field values [57].

3. NANOPARTICLE ADDITIONS

The addition of nanoparticles is a relatively straightforward method for industry to consider because of the potential ease of compatibility with YBCO processing. Several groups have demonstrated improved flux pinning with nanoparticle additions at near-standard processing temperatures of ~775°C, rather than higher temperatures where the buffer layer architectures might be compromised: Y211, Y_2O_3 or X nanoparticles or nanolayer additions by pulsed laser deposition (PLD) [60-72], $BaZrO_3$ (BZO) by PLD [72-74], $(Y,X)_xO_y$ by MOCVD [75,76], and $(Y,X)O_2$ or BZO by MOD [77,78].

The progress of J_c increases with nanoparticle additions by PLD is shown in figure 5, where J_c was measured only by magnetic methods (J_{cm}). In figure 5 only a few materials systems could be compared, since many authors used different magnetic ramping methods or

only measured J_c properties by transport methods or at slightly different temperatures of 75.5K [61-72]. In figure 5 significant improvements have been obtained, that vary depending on the field applied and temperature. At 77K 0.1T several materials including CeO_2, Y211 and La211 in (X/123)xN structures provided large improvements, whereas other materials provided minor increases or decreased J_c. Also results from figure 2 indicate that mixed $(Y_{1-x}Eu_x)123$ films provided strong enhancements at 77K 0.1 T, even slightly increased compared to CeO_2 and Y211 multilayer additions. However for those films, nanoparticle formation is small and may not be the controlling factor.

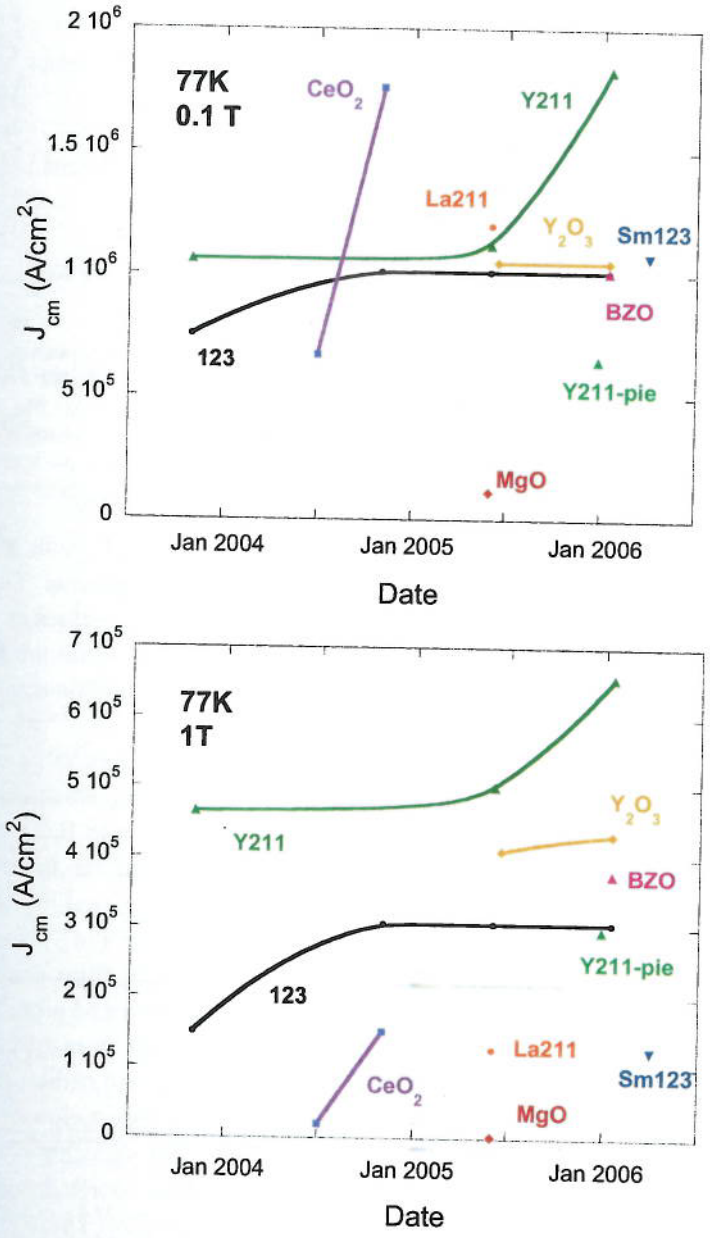

Figure 5. Continued on next page.

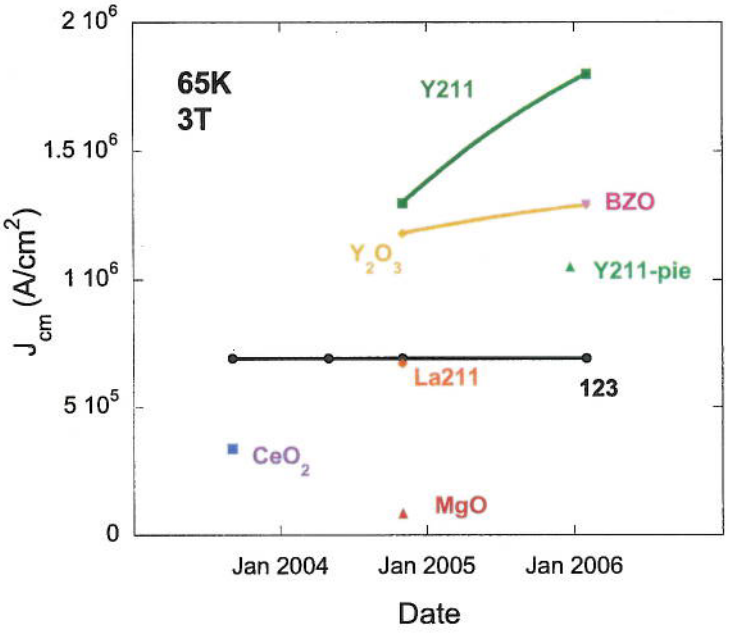

Figure 5. Progress in magnetic J_c achieved in $(X_{\sim 1nm}/123_{\sim 20nm})xN$ multilayer films deposited on single crystal substrates at 77K 0.1 T, 77K 1 T and 65K 3T as function of publication date [61-72]; BZO film is 2% volume fraction addition in a mixed single composition target [72]; the angular $J_c(H,1T)$ of this film lacked a c-axis peak suggesting the PLD conditions (775°C and 4 hz, 248 nm laser, 6 cm target-to-substrate distance) were not optimized for columnar growth obtained by other authors [73]. In figure 5 Y211-pie is pulsed laser deposition of a pie-shaped target [68]. Data of Sm123 is for a $(Sm123_{\sim 1.8nm}/123_{\sim 14.nm})x18$ multilayer film.

At 77K, the results at 1T are significantly different from 0.1T, with Y211 and Y_2O_3 multilayers and ($Y123_{0.98}BZO_{0.02}$) films providing strong enhancements. Other multilayer additions significantly reduced the J_c as much as 2x or more; in some cases as a consequence of severe degradation of T_c [65]. At 65K 3T, the J_c enhancements again are different again, with the Y211 pie method also providing J_c enhancement in addition to materials that provided strong pinning at 77K 1T.

The increase of J_c for films deposited only onto single crystal substrates are compared in figure 6. Both 211-multilayer and BZO additions provided strong enhancements on these substrates, however 211 had stronger increases at $H < 4$ T, while BZO provided larger enhancements for $H > 4T$. In figure 6 the films were in the range of 0.2-.0.3 microns. Results in the literature with larger film thickness ~ 1.0 μm were not compared in figure 6 since the intrinsic J_c is lower for these films typically by almost one half [74]. Results with Y_2O_3 additions were different depending on the experimental conditions; films deposited at ORNL showed obtained stronger improvement with 130 nm film thickness and probably larger Y_2O_3 nanoparticle size ~5-15 nm (width) and ~6nm (height) than results from AFRL with possible 2nm height [66,69,72]. The results by AFRL for Y_2O_3 additions are similar to earlier results with Y_2O_3-rich films made by MOCVD with small Y_2O_3 nanoparticle size ~ 5 nm [76]. Results by AFRL for $(Y_2O_3/123)xN$ multilayer films were not significantly different from 123 films (and were consistently obtained), in strong contrast to results for (211/123)xN additions which showed consistently strong increases [60,61,66,72]. These combined results suggest that either the Y_2O_3 nanoparticle size, film thickness, and or deposition conditions are

playing important roles in the pinning strengths obtained. Samples by AFRL for Y_2O_3 or 211 additions were obtained with exactly similar deposition conditions, except different layer parameters to optimize flux pinning [60,61,66,72].

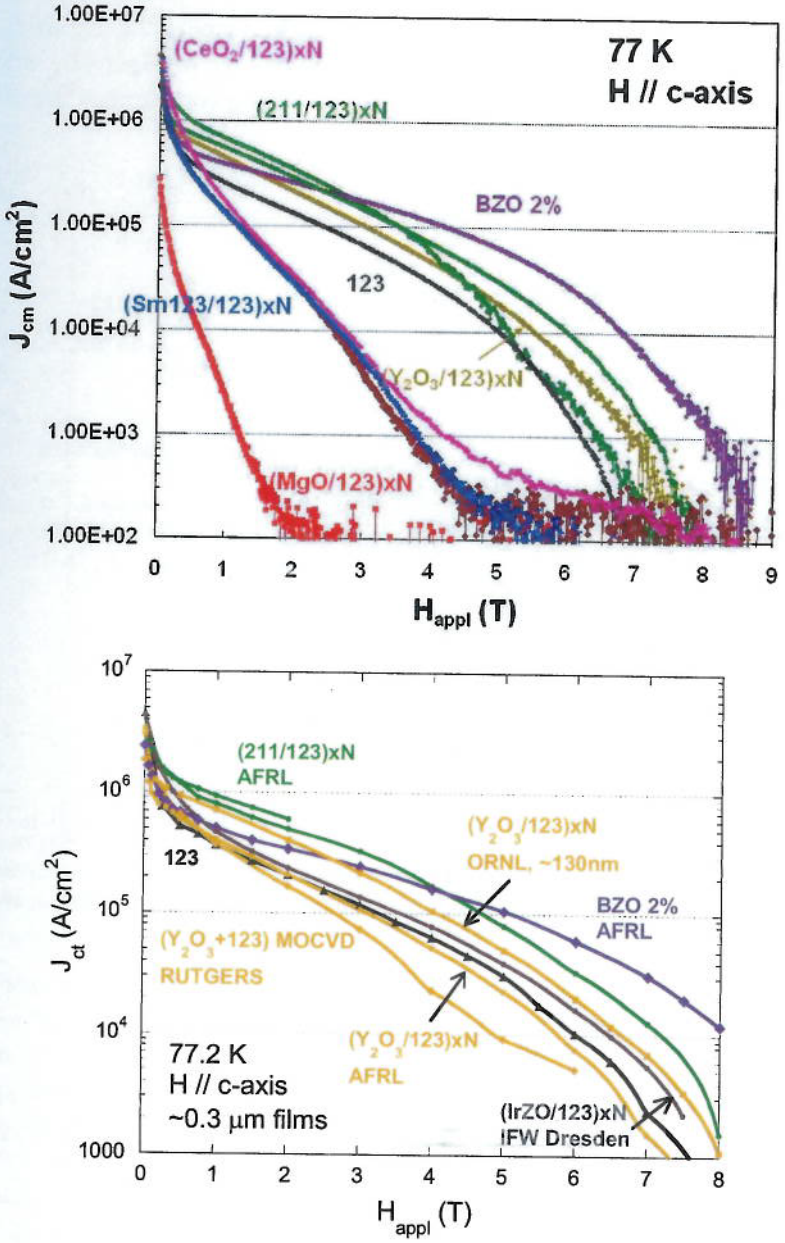

Figure 6. Comparison of (upper) magnetic J_c (J_{cm}) and (lower) transport J_c (J_{ct}) of thin films deposited on single crystal substrates for ($211_{\sim 1nm}/123_{\sim 20nm}$)xN multilayer [61,72], ($Y123_{0.98}BZO_{0.02}$) [72], (Y_2O_3/123)xN multilayer [72], (Y_2O_3/123)xN multilayer [69], (Y_2O_3+123) by MOCVD [76], (IrZO/123)xN multilayer (by reaction with Ir) [70], and 123 reference [72]. All films were deposited by PLD except as noted. Results from AFRL are representative and consistent for H < 5 T for 2 or 3 different samples; J_c(H) results > 5 T are less consistent.

Figure 7 provides additional information about pinning mechanisms by comparing transport J_c (J_{ct}) results on (RABIT's or IBAD) buffered-metallic substrates. In figure 7 a number of different methods produce strong pinning, including BZO 5%, BZO 2%, (211/123)xN multilayer tapes, and ($Y_{0.9}Sm_{0.1}$)123 films made by MOCVD. Results measured at 75.5 K are expected to have flatter dependence because of the lower measurement temperature, however the results suggests that nearly comparable improvements were obtained for 2% and 5% BZO additions (for example). In figure 7, normalized J_c measurements were compared, since the self-field J_cs varied considerably depending on the processing conditions, sample thickness, etc…

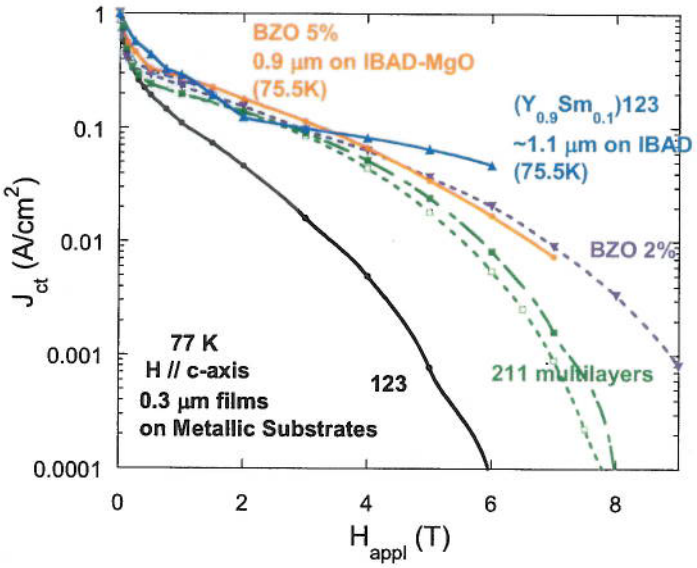

Figure 7. Comparison of transport J_c (J_{ct}) achieved on buffered metallic substrates for ($211_{\sim 1nm}/123_{\sim 20nm}$)xN multilayer tapes [67], ($Y123_{0.98}BZO_{0.02}$) composition films [73], ($123_{0.95}BZO_{0.05}$) [74], (Y0.9Sm0.1)123 [75], and ($123_{0.98}BZO_{0.02}$) [73]; the 123 reference is from Haugan et al. [67]. All films were deposited by PLD except for Sm-doped 123 which grown by MOCVD [75]. Note several samples were thicker and measured at 75.5K, which slightly affects the J_c(H) comparisons.

A comparison of J_c(77K,2T) pinning results on single crystal substrates are summarized as a function of lattice mismatch in figure 8 and 9, using data from figure 6 and additional samples analyzed [72]. In figures 8 and 9, J_c was measured by both magnetic and transport methods. For Y123 films, J_{ct}(77K,2T) ~ 0.2 MA/cm^2 were achieved which agrees almost exactly with similar measurements by other references of J_{ct}(77K,2T) ~ (0.15–0.2) MA/cm^2 [61,69,70] and indicates these samples are good references to measure the effects of flux pinning additions. Figures 8 and 9 indicates that the strongest pinning improvements are obtained only for high lattice mismatch phases Y211 and BZO, and additionally only 'non-reactive' materials providing effective pinning in experiments thus far. 'Reactive' materials may also pin, however the volume percentage would presumably have to be reduced quite low and has not been studied in great detail yet. Results for $BaIrO_3$ may have been compromised slightly since Ir was used as the addition which reacted with Ba in Y123 and probably reduced the superconducting volume percentage to some degree and produced secondary Y_2O_3 particles [70].

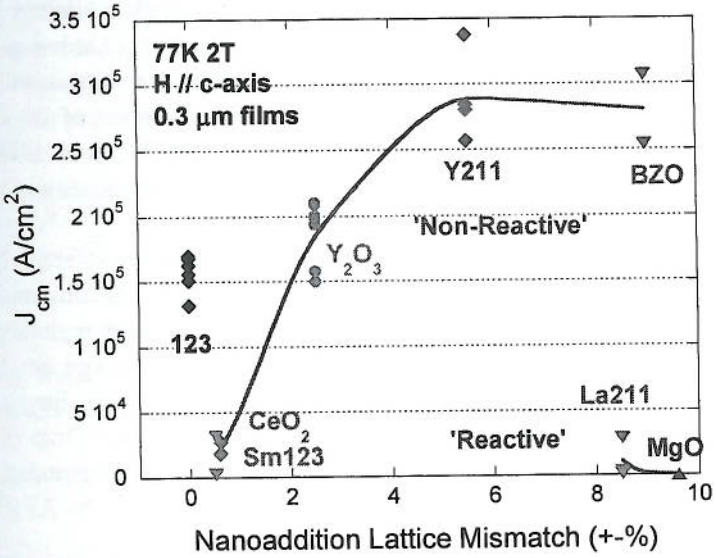

Figure 8. J_{cm} of films deposited on single crystal substrates; data is from samples in Figure 6 and additional samples [72]. Samples were all made at AFRL by PLD [61,72]. Films were $(M_{x\text{-}nm}/123_{y\text{-}nm})$xN multilayers with x = (0.3 nm to 1.8 nm) for the insulating 'pseudo-layer' and y = 3-20 nm for the 123 layer, except BZO which was from a $(BZO_{0.02}123_{0.98})$ single target. The curve fit is for 'non-reactive' phases indicating minimal reaction for (750°C-780°C) reaction temperatures.

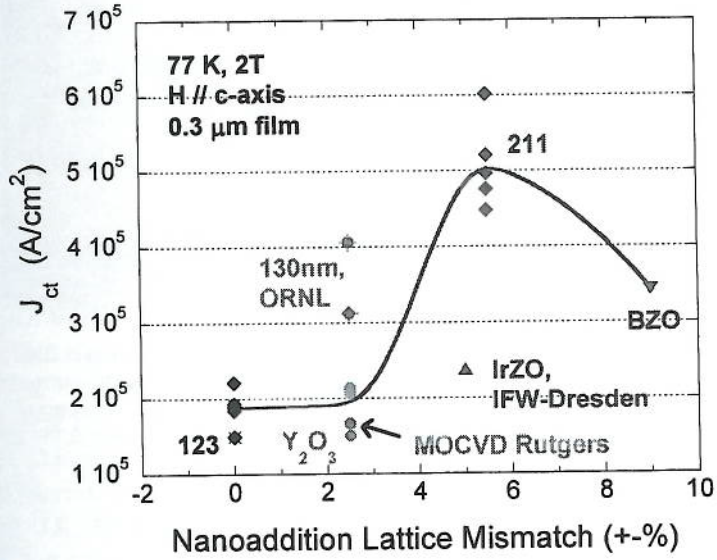

Figure 9. J_{ct} of films deposited on single crystal substrates; data is from figure 6, additional samples [72], and includes reference values for 123 from ORNL [69] and IFW-Dresden [70] marked as with solid-diamond + X. Samples not extra-marked were made at AFRL [61,72], and the curve fit is for these samples. All films were deposited by PLD except as noted in the figure and in the figure 6 caption.

In figure 9 a (2.5x-3x) improvement is obtained with Y211 multilayer additions [61,72] for a large range of magnetic field values ~ 0.5 T to 8T. At higher fields or other processing conditions (2%-5%) BZO also gives large increases, as shown in figures 6 and 7. Interestingly

in figure 6 and 8 the maximum increase for J_{cm} is about 2x which is slightly lower compared to the increase of J_c measured by transport methods of (2.5x-3x). This is a result of the more stringent criteria for J_{cm} measurements. The increase of critical current density with Y211 or BZO additions is a preferred method to increase the critical current of the tape, rather than other increasing the thickness of a lower current density tape [79]. It is difficult to maintain high J_c with increasing film thickness, and thicker films add to materials and processing costs [79].

The reason why high lattice mismatch phases are pinning more effectively is unknown at present, however it's suspected the effective volume of the nanoadditions is an important factor. A TEM micrograph shown in figure 10 indicates that stress regions surrounding the Y211-type nanoparticles especially in the c-axis direction are as large as 10-15 nm, which presumably increases the effective flux pinning volume flux pinning. Stress regions around Y_2O_3 nanoparticles are not as noticeable or smaller only extending ~ 2nm or so [76], which reduces their effective particle size apparently to the point where flux pinning is not improved as suggested by the non-pinning results in figure 8 for Y_2O_3 additions by AFRL.

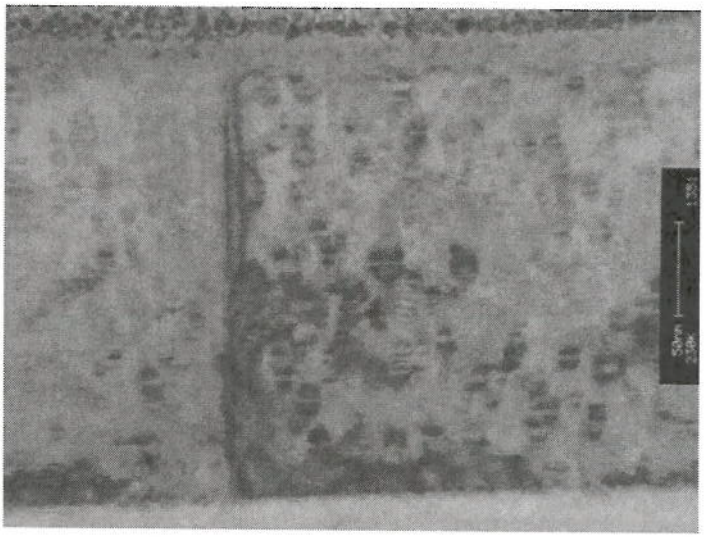

Figure 10. TEM micrograph of a $((Y_{0.9}Ca_{0.1})_2BaCuO_{5-z\sim0.5nm}/123_{\sim10nm})xN$ multilayer film deposited at 825°C. Note the nanoparticles are typically ~ 2nm thickness and 'stressed' shaded regions surrounding the nanoparticles extend almost 10-15nm in the c-axis direction. This is similar to micrographs of a ~ same dimension multilayer film without Ca substitution deposited at 775°C [80], however the stressed regions shown herein extend slightly farther.

SUMMARY

Several methods of in-situ flux pinning were reviewed, including nanoparticle additions and rare-earth substitutions. The results were compiled using already published or publicly available data. Thus far, rare-earth substitutions have provided substantial J_c increases at low-field $H < 1T$, whereas nanoparticle pinning has provided enhancements in the full range however mostly in high-fields $H > 1T$. For rare-earth substitution, a peak in J_c for $RE = 0.3$ was not observed for every (Y,RE)123 system reviewed, however there were some

enhancements observed with RE substitution. For nanoparticle pinning only large mismatch materials have provided consistent increases of J_c. For nanolayer materials such as Y_2O_3 additions with low mismatch ~ 2%, the results were seemingly dependent on processing conditions and most probably particle size; only large particles ~ 5 nm to ~ 50 nm nm in size gave enhancements [69,75,77,78] whereas other authors are reporting no increases of J_{ct} with most-probably smaller nanoparticles as shown herein.

ACKNOWLEDGEMENTS

The authors would like to express appreciation to the Air Force Office of Scientific Research and Air Force Research Laboratory – Propulsion Directorate for support of this work.

REFERENCES

[1] J.G. Bednorz and K.A. Muller, *Z. Phys. B.* 64, 189-193 (1986).
[2] M.K. Wu, J.R. Ashburn, C.J. Torng, P.H. Hor, R.L. Meng, L. Gao, Z.J. Huang, Y. Q. Wang and C.W. Chu, *Phys. Rev. Lett.* 58, 908-910 (1987).
[3] D. Larbalestier, A. Gurevich, D. Matthew Feldmann, A. Polyanskii, *Nature.* 414, 368-377 (2001).
[4] T. Matsushita, *Supercond. Sci. Technol.* 13, 730-737 (2000).
[5] L. Civale, A.D. Marwick, T.K. Worthington, M.A. Kirk, J.R. Thompson, L. Krusin-Elbaum, Y. Sun, J.R. Clem, and F. Holtzberg, *Phys. Rev. Lett.* 67, 648-651 (1991).
[6] M. T. Maladievsky, C. A. D'Ovidio, Supercond. Sci. Tech. 18(3), 289-293 (2005).
[7] V. Selvamanickam, H.G. Lee, Y. Li, X. Xiong, Y. Qiao, J. Reeves, Y. Xie, A. Knoll, and K. Lenseth, *Physica C.* 392-396, 859-862 (2003).
[8] D.T. Verebelyi, U. Schoop, C. Thieme, X. Li, W. Zhang, T. Kodenkandath, A.P. Malozemoff, N. Nguyen, E. Siegal, D. Buczek, J. Lynch, J. Scudiere, M. Rupich, A. Goyal, E.D. Specht, P. Martin, and M. Paranthaman, *Supercond. Sci. Technol.* 16, L19-L22 (2003).
[9] J.R. Groves, P.N. Arendt, S.R. Foltyn, Q. Jia, T.G. Holesinger, H. Kung, R.F. DePaula, P.C. Dowden, E.J. Peterson, L. Stan, and L.A. Emmert, *Physica C.* 382, 43-47 (2002).
[10] A. Goyal, D.F. Lee, F.A. List, E.D. Specht, R. Feenstra, M. Paranthaman, X. Cui, S.W. Lu, P.M. Martin, D.M. Kroeger, D.K. Christen, B.W. Kang, D.P. Norton, C. Park, D.T. Verebelyi, J.R. Thompson, R.K. Williams, T. Aytug, and C. Cantoni, *Physica C.* 357-360, 903-913 (2001).
[11] U. Balachandran, B. Ma, M. Li, B.L. Fisher, R.E. Koritala, D.J. Miller, S.E. Dorris, *Physica C.* 392-396(2), 806-814 (2003).
[12] K. Kakimoto, Y. Iijima, T. Saitoh, *Physica C.* 392-396(2), 783-789 (2003).
[13] H. Yamasaki, Y. Nakagawa, A. Sawa, H. Obara, K. Develos, *Physica C.* 372-376, 1885-1889 (2002).
[14] P. N. Barnes, M. D. Sumption, G. L. Rhoads, *Cryogenics.* 45, 670-686 (2005).

[15] Y. Feng, A. K. Pradhan, Y. Zhao, Y. Wu, N. Koshizuka, and L. Zhou, "Influence of Ho substitution for Y on flux pinning in melt-processed YBCO superconductors," *Physica C.* 357-360,799-802 (2001).

[16] V. Selvamanickam, Y. Xie, J. Reeves, and Y. Chen, "MOCVD-Based YBCO-Coated Conductors," *MRS Bulletin.* August 2004, 579-582 (2004).

[17] K. Matsumoto, D. Takahara, T. Horide, A. Ichinose, S. Horii, Y. Yoshida, M. Mukaida, and K. Osamura, "High-J_c Gd-Ba-Cu-O Epitaxial Films Prepared by Pulsed Laser Deposition," *IEEE Trans. Appl. Supercond.* 15(2), 2719-2722 (2005).

[18] G. Osabe, T. Takizawa, S.I. Yoo, N. Sakai, T. Higuchi, M. Murakami, "Studies of the $Nd_{1+z}Ba_{2-x}Cu_3O_y$ solid solutions," *Mat. Sci. Engineer.* B65, 11-16 (1999).

[19] H. H. Wen, Z. X. Zhao, Y. G. Xiao, B. Yin, and J. W. Li, "Evidence for flux pinning induced by spatial fluctuation of transition temperatures in single domain $(Y_{1-x}Pr_x)Ba_2Cu_3O_{7-\delta}$ samples," *Physica C.* 251, 371-378 (1995).

[20] E. S. Reddy, P. V. Patanjali, E. V. Sampathkumaran, R. Pinto, "Fabrication and superconducting properties of ternary $REBa_2Cu_3O_y$ thin films," *Physica C.* 366, 123-128 (2002).

[21] M. R. Koblischka, M. Muralidhar, M. Murakami, "Flux pinning sites in melt-processed $(Nd_{0.33}Eu_{0.33}Gd_{0.33})Ba_2Cu_3O_y$ superconductors," *Physica C.* 337, 31-38 (2000).

[22] M. Jirsa, M. R. Koblischka, T. Higuchi, M. Muralidhar, M. Murakami, "Comparison of different approaches to modeling the fishtail shape in RE-123 bulk superconductors," *Physica C.* 338, 235-245 (2000).

[23] C. Varanasi, P. J. McGinn, H. A. Blackstead, and D. B. Pulling, "Nd Substitution in Y/Ba Sites in Melt Processed $YBa_2Cu_3O_{7-\delta}$ Through Nd_2O_3 Additions," *Journal of Electronic Materials.* 24[12], 1949-1953 (1995).

[24] D. N. Matthews, J. W. Cochrane, G. J. Russell, "Melt-textured growth and characterization of a $(Nd/Y)Ba_2Cu_3O_{7-\delta}$ composite superconductor with very high critical current density," *Physica C.* 249, 255-261 (1995).

[25] P. Schätzle, W. Bieger, U. Wiesner, P. Verges and G. Krabbes, "Melt Processing of (Nd,Y)BaCuO and (Sm,Y)BaCuO composites," *Supercond. Sci. and Technol.* 9, 869-874 (1996).

[26] A. S. Mahmoud and G. J. Russell, "Large crystals of the composite Y/Nd(123) containing various dopants grown by melt-processing in air," *Supercond. Sci. and Technol.* 11, 1036-1040 (1998).

[27] X. Yao, E. Goodilin, Y. Yamada, H. Sato and Y. Shiohara, "Crystal growth and superconductivity of $Y_{1-x}Nd_xBa_2Cu_3O_{7-\delta}$ solid solutions," *Applied Superconductivity.* 6[2-5], 175-183 (1998).

[28] D. K. Aswal, T. Mori, Y. Hayakawa, M. Kumagawa, "Growth of $Y_{1-z}Nd_zBa_2Cu_3O_x$ single crystals," *Journal of Crystal Growth.* 208, 350-356 (2000).

[29] H. Wu, K. W. Dennis, M. J. Kramer, and R. W. McCallum, "Solubility Limits of $LRE_{1+x}Ba_{2-x}Cu_3O_{7+\delta}$," *Applied Superconductivity.* 6[2-5], 87-107 (1998).

[30] T. J. Haugan, M. E. Fowler, J. C. Tolliver, P. N. Barnes, W. Wong-Ng, L. P. Cook, "Flux Pinning and Properties of Solid-Solution $(Y,Nd)_{1+x}Ba_{2-x}Cu_3O_{7-\delta}$ Superconductors", in *Processing of High Temperature Superconductors*, Ceramic Transactions Vol. 104, edited by A. Goyal, W. Wong-Ng, M. Murakami, J. Driscoll (American Ceramic Society, Westerville OH, 2003), p. 299 - 307.

[31] T. J. Haugan, J. M. Evans, J. C. Tolliver, I. Maartense, P. N. Barnes, W. Wong-Ng, L. P. Cook, R.D. Shull, "Flux Pinning and Properties of Solid-Solution $(Y,Nd)_{1+x}Ba_{2-x}Cu_3O_{7-d}$ Superconductors Processed in Air and Partial Oxygen Atmospheres" in *Fabrication of Long-Length and Bulk High Temperature Superconductors,*, Ceramic Transactions Vol. 149, edited by R. Meng, A. Goyal, W. Wong-Ng, H.C. Freyhardt, and K. Matsumoto (American Ceramic Society, Westerville OH, 2004), p. 151 – 162.

[32] R. W. McCallum, M. J. Kramer, K. W. Dennis, M. Park, H. Wu, and R. Hofer, "Understanding the Phase Relations and Cation Disorder in $LRE_{1+x}Ba_{2-x}Cu_3O_{7+\delta}$," *J. of Electr. Mater.* 24[12], 1931-1935 (1995).

[33] J. L. MacManus-Driscoll, S. R. Foltyn, Q. X. Jia, H. Wang, A. Serquis, B. Maiorov, L. Civale, Y. Lin, M. E. Hawley, M. P. Maley, D. E. Peterson, "Systematic enhancement of in-field critical current density with rare-earth ion size variance in superconducting rare-earth barium cuprate films," *Appl. Phys. Lett,* 84, 5329-5331 (2004).

[34] J. L. MacManus-Driscoll, S. R. Foltyn, B. Maiorov, Q. X. Jia, H. Wang, A. Serquis, L. Civale, Y. Lin, M. E. Hawley, M. P. Maley, D. E. Peterson, "Rare earth ion size effects and enhanced critical current densities in $Y_{⅔}Sm_{⅓}Ba_2Cu_3O_{7-x}$," *Appl. Phys. Lett.* 86, 032505-032507 (2005).

[35] Y. Li, Z.-X. Zhao, "Stress-field pinning induced by the lattice mismatch in 123 phase," *Physica C.* 351 , 1-4 (2001).

[36] Y. Li, L. Cui, G. Cao, Q. Ma, C. Tang, Y. Wang, L. Wei, Y. Z. Zhang, Z. X. Zhao, E. Baggio-Saitovitch, "Positron annihilation study on the stress-field pinning mechanism in (Eu,Y)-123 superconductors," *Physica C.* 314, 55-68 (1999).

[37] Y. Shiohara, A. Endo, "Crystal growth of bulk high-T_c superconducting oxide materials," *Mater. Sci. Engineer,* R19, 1-86 (1987).

[38] J. M. S. Skakle, "Crystal chemical substitutions and doping of $YBa_2Cu_3O_x$ and related superconductors," *Mater. Sci. Engineer.* R23, 1-40 (1998).

[39] J. L. MacManus-Driscoll, "Materials Chemistry and Thermodynamics of $REBa_2Cu_3O_{7-x}$ " *Adv. Mater.*, 9, 457-473 (1997).

[40] T. J. Haugan, J. C. Tolliver, J. M. Evans, J. W. Kell, "Crystal Chemical Substitutions of $YBa_2Cu_3O_{7-\delta}$ To Enhance Flux Pinning", in HTS Thin Film and More on Vortex Studies (Studies of High Temperatures Superconductors, Volume 49) (Ed. A. Narlikar), Nova Sci. Publishers, NY (2005).

[41] X.W. Cao, X.J. Xu, Z.H. Wang, J. Fang, R.L. Wang, H.C. Li, "Properties of upper critical field and pinning potential in epitaxial $GdBa_2Cu_3O_{7-\delta}$," *Physica C.* 282-287, 1993-1994 (1997).

[42] L. Bejjit, A. Deville, M. Haddad, B. Gaillard, H. Noel, O. Monnereau, "Gadolinium Substitution for Yttrium and Chemical Preparation Effects in $YBa_2Cu_3O_7$: An EPR Study," *Ann. Chim. Sci. Mat.*, 23, 217-220 (1998).

[43] Y. Feng, L. Zhou, J.G. Wen, N. Koshizuka, A. Sulpice, J.L. Tholence, J.C. Vallier, P. Monceau, "Fishtail effect, magnetic properties and critical current density of Gd-added PMP YBCO," *Physica C*, 297, 75-84 (1998).

[44] G. F. Goya, "Magnetic Properties of the solid solution $(Y_{1-x}Gd_x)_2BaCuO_5$ $(0 \le x \le 1)$," *J. Mag. and Magn. Mat.*, 205, 215-220 (1999).

[45] V.N. Narozhnyi, V.N. Kochetkov, "Influence of rare-earth ionic radius on the properties of Ni- and Fe-substituted R $Ba_2(Cu_{1-x}M_x)O_{7-y}$ systems (R=Y,Nd,Eu,Gd,Ho,Tm; *M*=Ni,Fe)," *Phys. Rev. B,* 53(9), 5856-5862 (1996).

[46] R.L.Wang, H.C. Li, B. Yin, J.W. Li, X.S. Ron, C. Dong, F. Wu, H. Chen, Z.X Zhao, "Critical current density and flux pinning in $Gd_{1-x}Y_xBa_2Cu_3O_{7-y}$ epitaxial thin films," *Physica C*, 250, 55-58 (1995).

[47] H.H. Wen, Z.X. Zhao, R.L.Wang, H.C. Li, B. Yin, "Evidence for the lattice-mismatch-stress-field induced flux pinning in $(Gd_{1-x}Y_x)Ba_2Cu_3O_{7-\delta}$ thin films", *Physica C*, 262, 81-88 (1996).

[48] Z.S. Peng, J.M. Hao, B. Yin, A.X. Zhao, Z.Q. Hua, B.C. Yang, "The Relationship of the Critical Current Density and the Lattice Deformation in $Y_{1-x}RE_xBa_2Cu_3O_{7-\delta}$ Epitaxial Films," *Physica C*, 282-287, 2103-2104 (1997).

[49] A.R. Devi, V.S. Bai, P.V. Patanjli, R. Pinto, N.H. Kumar, S.K. Malik, "Enhanced critical current density due to flux pinning from lattice defects in pulsed laser ablated $Y_{1-x}Dy_xBa_2Cu_3O_{7-\delta}$ thin films", *Supercond. Sci. Technol.* 13, 935-939 (2000).

[50] Y. Li, G. K. Perkins, A. D. Caplin, G. Cao, Q. Ma, L. Wei, Z. X. Zhao, "Study of the pinning behavior in yttrium-doped Eu-123 superconductors," *Supercond. Sci. Technol.* 13, 1029-1034 (2000).

[51] W. Wong-Ng, et. al., private communication and presented at *DOE Peer Reviews,* 2000-2005.

[52] J. Shimoyama, Univ. of Tokyo, *private communication,* 2003.

[53] Z. Chen, Y. Xue, Y. Su, J. Jin and Z. Tian, "Influence of Gd/Eu substitution on the local electron density and the superconductivity of $Y_{1-x}RE_xBa_2Cu_3O_{7-\delta}$ (R=Gd,Eu) systems," presented at CEC-ICMC, Keystone CO Sept. 2005.

[54] L. Cao and J. Zegenhagen, *Phys. Stat. Sol.* B 215, 587-590 (1999).

[55] Y. C. Liao, W. Guan, M. K. Wu, Y.-D. Chiu, C. C. Chi, *Supercond. Sci. Technol.* 13, 1090-1094 (2000).

[56] Q. X. Jia, S. R. Foltyn, P. N. Arendt, H. Wang, J. L. MacManus-Driscoll, Y. Coulter, Y. Li, M. P. Maley, and M. Hawley, *Appl. Phys. Lett.* 83(7), 1388-1391 (2003).

[57] T. J. Haugan, T. A. Campbell, I. Maartense, C. V. Varanasi, P. N. Barnes, presented at MRS Spring 2005 Conference and CEC-ICMC 2005, and to submit for publication.

[58] C. V. Varanasi, J. C. Tolliver, T. J. Haugan, S. Sathiraju, I. Maartense, and P. N. Barnes, *IEEE Trans. Appl. Supercond.* 15(2), 3722-3724 (2005).

[59] T. J. Haugan, J. M. Evans, I. Maartense, P. N. Barnes, submitted to Ceramics Transactions, Oct. 2005.

[60] T. Haugan, P.N. Barnes, I. Maartense, E. J. Lee, M. Sumption, C. B. Cobb, *J. Mat. Res.* 18 (2003) 2618-2623.

[61] T. Haugan, P.N. Barnes, R. Wheeler, F. Meisenkothen, M. Sumption, *Nature.* 430, 867-870 (2004).

[62] P. N. Barnes, T. J. Haugan, M. D. Sumption, S. Sathiraju, J. M. Evans, J. C. Tolliver, *Trans. Mat. Res. Soc.* Japan 29(4), 1385-1388 (2004).

[63] P. N. Barnes, T. J. Haugan, C. V. Varanasi, T. A. Campbell, *Appl. Phys. Lett.* 85(18), 4088-4090 (2004).

[64] T. Haugan, P. Barnes, R. Nekkanti, J. M. Evans, L. Brunke, I. Maartense, J. P. Murphy, A. Goyal, A. Gapud, and L. Heatherly, in "Epitaxial Growth of Functional Oxides, Ed.

by A. Goyal, Y. Kuo, O. Leonte, and W. Wong-Ng, (The Electrochemical Society Inc., Pennington NJ 2005), p.359-366.

[65] T. J. Haugan, P. N. Barnes, T. A. Campbell, J. M. Evans, J. W. Kell, L. B. Brunke, J. P. Murphy, C. Varanasi, I. Maartense, W. Wong-Ng, L. P. Cook, *IEEE Trans. Appl. Supercond.* 15(2), 3770-3773 (2005).

[66] T. A. Campbell, T. J. Haugan, I. Maartense, J. Murphy, L. Brunke, and P.N. Barnes, *Physica C.* 423, 1-8 (2005).

[67] T. J. Haugan, P.N. Barnes, T.A. Campbell, A. Goyal, A. Gapud, L. Heatherly, S. Kang, *Physica C.* 425, 21-26 (2005).

[68] C. Varanasi, P. N. Barnes, J. Burke, J. Carpenter, T. J. Haugan, *Appl. Phys. Lett.* 87, 262510-262512 (2005).

[69] A.A. Gapud, D. Kumar, S.K. Viswanathan, C. Cantoni, M. Varela, J. Abiade, S.J. Pennycook and D.K. Christen, *Supercond. Sci. Technol.* 18, 1502-1505 (2005).

[70] J. Hänisch, C. Cai, R. Huhne, L. Schultz, and B. Holzapfel, *Appl. Phys. Lett.* 86, 122508-122510 (2005).

[71] R.L.S. Emergo, J. Wu, T.J. Haugan, and P. N. Barnes, *Appl. Phys. Lett.* 87, 232503-232505 (2005).

[72] T.J. Haugan, P.N. Barnes, T.A. Campbell, N. Pierce, J.W. Kell, M.F. Locke, S. Sathiraju, I. Maartense and R. Wheeler, Proceedings of CCA-2005, to appear Jan 2006 on CD.

[73] A. Goyal, S. Kang, K.J. Leonard, P.M. Martin, A.A. Gapud, M. Varela, M. Paranthaman, A. O. Ijaduola, E.D. Specht, J.R. Thompson, D.K. Christen, S.J. Pennycook, and F.A. List, *Supercond. Sci. Technol.* 18, 1533-1538 (2005).

[74] J. L. MacManus-Driscoll, S. R. Foltyn, Q.X. Jia, H. Wang, A. Serquis, L. Civale, B. Maiorov, M.E. Hawley, M.P. Maley, and D.E. Peterson, *Nature Mat.* 3, 439-443 (2004).

[75] V. Selvamanickam, Y. Xie, J. Reeves, and Y. Chen, *MRS Bull.* August, 579-582 (2004).

[76] P. Lu, Q. Li, J. Zhao, C.S. Chem, B. Gallois, P. Norris, B. Kear, F. Cosandey, *Appl. Phys. Lett.* 60(10), 1265-1267 (1992).

[77] U. Schoop, M. W. Rupich, C. Thieme, D. T. Verebelyi, W. Zhang, X. Li, T. Kodenkandath, N. Nguyen, E. Siegal, L. Civale, T. Holesinger, B. Maiorov, A. Goyal, and M. Paranthaman, *IEEE Trans. Appl. Supercond.* 15(2), 2611-2616 (2005).

[78] N. Long, N. Strickland, B. Chapman, N. Ross, J. Xia, X. Li, W. Zhang, T. Kodenkandath, Y. Huang, and M. Rupich, *Supercond. Sci. Technol.* 18, S405-S408 (2005).

[79] M. Rupich, American Superconductor Corporation, DOE Coated Conductor Workshop, Jan 2006.

[80] T. Holesinger, Los Alamos National Laboratory, *private communication,* Jan. 2005.